Estimation of nitrate nitrogen content in cotton petioles under drip irrigation based on spectral indices and wavelet neural network

Zhiqiang Dong (✉ shuaidadada@126.com)

Shihezi University College of Agriculture   https://orcid.org/0000-0002-6003-6895

Yang Liu

Shihezi University College of Agriculture

Baoxia Ci

Shihezi University College of Agriculture

Ming Wen

Shihezi University College of Agriculture

Minghua Li

Shihezi University College of Agriculture

Xi Lu

Shihezi University College of Agriculture

Xiaokang Feng

Shihezi University College of Agriculture

Shuai Wen

Shihezi University College of Agriculture

Fuyu Ma

Shihezi University College of Agriculture

Abstract

Background: Estimating nitrate nitrogen (NO_3^--N) content in petioles is one of the key approaches for monitoring nitrogen (N) nutrition in crops. Rapid, non-destructive, and accurate monitoring of great NO_3^--N content in cotton petioles under drip irrigation is of great significance.

Methods: NO_3^--N content in cotton petioles under drip irrigation and the corresponding canopy spectral reflectance of cotton plants grown in experimental plots under various N application levels were analyzed. The correlations among 'trilateral parameters' and six vegetation indices, and NO_3^--N content in petioles were determined. A traditional regression model of NO_3^--N content in cotton petioles under drip irrigation was established, and a wavelet neural network (WNN) model with different index numbers was developed. The WNN model was verified using independent data, and compared with the random forest algorithm , radial basis function neural network and back propagation neural network.

Results: Based on the analyses of 'trilateral parameters' and petiole NO_3^--N content, blue edge amplitude (Db) and blue edge area (SDb) of the blue edge parameters exhibited a strong positive correlation with petiole NO_3^--N content, and the correlation coefficients was 0.90. Among the blue edge parameters, the coefficient of determination (R^2) of the Db polynomial regression equation and petiole NO_3^--N content was the highest (R^2 = 0.89), while the root mean square error (RMSE) of the linear regression model was the lowest (RMSE = 1.04). R^2 value of the traditional regression model developed using blue edge parameters and petiole NO_3^--N content significantly increased, while RMSE value decreased when compared with those of the red edge and yellow edge parameters. Analyses results of the vegetation index developed using original spectral reflectance data and the vegetation index developed using the first set of derivative spectral reflectance data and petiole NO_3^--N content, revealed that the first derivative vegetation index, normalized difference spectral index (ND705) exhibited a strong negative correlation, with a correlation coefficient of -0.90. The first derivative vegetation index, ND705 and petiole NO_3^--N content index regression equation had the highest coefficient of determination (R^2 = 0.83), while the first derivative vegetation index, red edge model index ($CI_{red-edge}$) and petiole NO_3^--N content linear regression equation had the lowest RMSE = 0.92. R^2 value of the traditional regression equation for the first derivative vegetation index and petiole NO_3^--N content significantly increased, while the RMSE value decreased when compared with the original spectral vegetation index. After conducting correlation analyses and developing traditional regression models, Db and SDb of the blue edge parameters, and the first derivative vegetation index, ND705 and $CI_{red-edge}$ were used to develop a WNN model. The model based on blue edge parameters had R^2 of 0.88, RMSE of 0.74g/L and mean absolute error (MAE) of 0.58 g/L, the R^2 value was 8.6% higher than the R^2 the first derivative vegetation index model, in which RMSE and MAE reduced by 18.7% and 20.5%, respectively. The model was tested using independent verification data, and which revealed that the R^2 value of the model was 0.88, RMSE was 0.65g/L, and MAE was 0.47g/L based on the blue edge parameters, predicted value of WNN, and true value of the verification

model, which was superior other models. The performance of the WNN model based on the blue edge parameters improved by 7.3%, and RMSE and MAE reduced by 25.2% and 30.9%, respectively when compared with those of the vegetation index model.

Conclusion: The present study demonstrated that an inexpensive approach consisting of WNN algorithm and spectrum can be used to enhance the accuracy of NO_3^--N content estimation in cotton petioles under drip irrigation, which reflects their practical application potential.

Background

Optimal management of nitrogen (N) fertilizer is of great significance to the improvement of yield and quality of cotton [1], and the reduction of waste and environmental problems caused by excessive N fertilizer input [2]. A reasonable amount of N fertilizer is conducive for the maintenance of a balance between vegetative growth in cotton, and promotion of N absorption and utilization efficiency [3, 4]. N fertilizer is generally stored and assimilated by cotton plants in the form of nitrate nitrogen (NO_3^--N). NO_3^--N content varies in different parts of the cotton plant, and follows the order of petioles > stems > leaves [5]. The relationships among cotton leaves, petioles, buds, and bolls reflect the coordinated relationship between vegetative and reproductive growth in cotton plants [6], which subsequently influence the yield and quality of cotton [7]. Therefore, petiole NO_3^--N content is an effective parameter that reflects the overall N nutrition status of cotton, and petioles can be used as primary plant parts in the diagnose N nutrition [8, 9]. Petioles also facilitate rapid determination of N nutrition status of plants to guide rational application of N fertilizer [10, 11].

The traditional methods of evaluating cotton N nutrition predominantly include soil mineral N determination, laboratory analysis of plant, determination of petiole NO_3-N, etc.; [12, 13] however, the methods are associated with certain demerits such as the procedures are cumbersome, time consuming, poor timing of analyses results, and they involve destructive sampling of numerous plants[14, 15]. Hyperspectral remote sensing technology has been widely used in the estimation of physiological parameters during crop growth and development due to its non-destructive, cheap, and efficiency characteristics [16]. The diagnosis of N nutrition in crops based on spectral data has made considerable progress [17]. The technique has been applied in several crops to rapidly obtain crop N nutrition status spectral indices derived from spectral [18–20]. Several researchers have developed crop N nutrition monitoring models based on spectral indices, and achieved high accuracy. Wang et al. [21] demonstrated that the ratio spectral index (RSI, 822,738) could be used as an indicator for monitoring N accumulation in rice and wheat leaves. Liu et al. [22] proposed a ratio vegetation index (RVI, 764,657) based on reflectance at wavelengths of 764 and 657 nm as an effective indicator of N status of oilseed rape in winter.

In addition, as the parameters associated with spectral location characteristics, 'trilateral parameters' cannot only reflect the spectral characteristics of vegetation, but are also sensitive to variations in N

content [23]. The red edge parameter, which is one of the 'trilateral parameters' has been successfully used to the estimate N nutrition in a variety of crops with satisfactory results [24, 25]. The red edge 'blue shift' phenomenon exists in the reflectance spectra of numerous crops. Railyan [26] and Gilbert [27] established that the position and red edge slope in triticale and maize varied constantly during the entire growing season, and were closely associated with the phonological period of crops. The red edge shifted to the long wave direction in the vegetative growth stage, and shifted to the short wave direction in the reproductive growth stage.

The spectral indices of crops can be obtained by developing linear or nonlinear relationship or learning method of artificial neural networks, and the application of spectral indices combined with artificial neural network algorithms to estimate N content has presented numerous research results. Feng et al. [28] established the quantitative estimation models of N content rice canopy leaves based on adaptive differential optimization extreme learning machine, radial basis function (RBF) and particle swarm optimization BP. To estimate the N content of maize in natural environments rapidly and accurately, Xiu et al. [29] proposed a method for measuring maize N content based on wavelet energy coefficient and back propagation neural network (BP). The method improved the accuracy of corn N content estimation when compared with the regression analysis model. Wavelet neural network (WNN) [30] is a type of an artificial neural network, which is generated by applying wavelet analysis theory to neural network theory, and exhibits strong nonlinear mapping and learning capabilities [30]. The current research on WNN covers several fields such as medicine [31], industry [32], and finance [33] and has achieved satisfactory results.

Presently, few studies have investigated the application of hyperspectral technology and WNN in the monitoring of NO_3^--N content in cotton petioles under drip irrigation. Therefore, the present study selected spectral indices and 'trilateral parameters' that are sensitive to N and used them to estimate the NO_3^--N content of cotton petioles based on the field experiments of cotton under drip irrigation, and various N application levels in Xinjiang. A combined WNN model, which has strong adaptive and fault tolerant abilities, can effectively estimate the advantages of linear and nonlinear functions, and facilitate the estimation of petiole NO_3^--N content in cotton under drip irrigation to provide technical references for cotton growth and N nutrition diagnosis under drip irrigation.

Methods

Experimental design

The field experiment was carried out in 2019 at the teaching test site of Shihezi University, Shihezi City, Xinjiang Uygur Autonomous Region(86°02'E, 44°18'N) (Fig. 1 a, b). Soil fertility in the 0-20 cm soil layer in the experimental plots was determined; total N was 1.13 g/kg, alkali-hydro N was 44.26 mg/kg, available phosphorus content was 19 mg/kg, available potassium content was 486 mg/kg, organic matter content was15.50 g/kg, pH value was 8.17. Lumianyan 24 cotton variety, which is middle-late maturing variety, with a growth period of approximately130 days was used as the experiment material.

Five N gradients were designed as follows: 0 kg/ha (N0), 195.5 kg/ha (N1), 299 kg/ha (N2), 402.5 kg/ha (N3) and 506 kg/ha (N4). The total amount of phosphate (P_2O_5) and potassium (K_2O) fertilizers were 109.8 kg/ha and 91.8 kg/ha, respectively. One film, three rows, and three belts were used in the experiment. The row spacing was 76 cm and the plant spacing was 10 cm. Each treatment was repeated three times and arranged in completely randomized blocks covering a plot area of 2.25m × 15m. Cotton is was first crop to be grown in the experimental field, and protective rows were set around the cotton plants. Other field management measures were in accordance with the requirements of high-yield cultivation. Fertilizers were applied with irrigation water during the cotton growth period under drip irrigation with film.

Validation test data were obtained from a high-yield cotton field in Shihezi University Teaching Experimental Field (Fig. 1c). The independent test cotton field was divided into 15 plots. The total amount of N fertilizer applied was 300 kg/ha, while the total amount of P_2O_5 and K_2O fertilizers applied were 109.8 kg/ha and 91.8 kg/ha, respectively.

Spectral data acquisition

The key growth period of cotton was divided as follows: full bud period (65 days after sowing), initial flowering period (77 days after sowing). full flowering period (88 days after sowing), and initial boll stage (107 days after sowing). Analytical Spectral Devices ASD FieldSpec 3 portable spectrometer (Analytical Spectral Devices Inc., Boulder, CO, Colorado, USA) was used to obtain spectral data of the cotton canopy. The band range was 350−1075 nm, and the field of view was 25°. Three rows of cotton plants with uniform growth in different treatment plots were randomly selected. The spectrometer probe was placed vertically downward at 25 cm above the canopy. The trigger was pulled during scanning and the spectral data obtained were automatically saved. The spectral data acquisition time was three hours. The average values of the three curves were calculated using 'ViewspecPro' software (Analytical Spectral Devices, Inc., Boulder, CO, Colorado, USA) as the reflectance values of the cell spectra.

Determination of NO_3^--Ncontent in cotton petioles

After the collection of canopy spectral data, 20 cotton plants with petioles (10 days after topping) and two leaves (10 days after topping) were randomly selected from the experimental. Cotton petioles and leaves were separated, the petioles were cut and pressed, and the sap was immediately measured using the 'LAQUA twin NO_3^- meter' (a brief description of NO_3^- meter is presented in Table 1).

Spectral parameter selection

Spectral indices were associated with cotton photosynthesis, soil fertility level, nutrient management, etc. Six spectral indices and 'trilateral parameters' that are sensitive to N nutrition in cotton under drip irrigation were selected based on the spectral response characteristics of cotton canopy under drip irrigation and previous studies, as shown in Table 2.

WNN, random forest (RF) algorithm, RBF, and BP were used to establish the estimation model of cotton petiole NO_3^--N content. Two spectral characteristic indices and two 'trilateral parameters' with strong correlation between critical growth period and petiole NO_3^--N content were selected as the independent variables to develop a cotton petiole NO_3^--N content model. Independent validation samples were used to test the regression model. The coefficient of determination (R^2), root mean square error (RMSE), and mean absolute error (MAE) were used to enhance the accuracy of the model to develop the best estimation model (Eqs. 1–3). The mean relative error (MRE) was used to determine the number of hidden nodes in WNN (Eq. 4).

$$R^2 = 1 - \frac{\sum_{i=1}^{n}(F_i - T_i)^2}{\sum_{i=1}^{n}(T_i - \bar{T_i})^2} \tag{1}$$

$$RMSE = \sqrt{\frac{1}{n} \times \sum_{i=1}^{n}(F_i - T_i)^2} \tag{2}$$

$$MAE = \frac{1}{n}\sum_{i=1}^{n}|F_i - T_i| \tag{3}$$

$$MRE = \sqrt{\frac{1}{n} \times \sum_{i=1}^{n}\left(\frac{F_i - T_i}{T_i}\right)^2} \times 100\% \tag{4}$$

Where Fi and Ti are the predicted and true values, respectively, and n is the number of samples.

Modeling method

WNN [42] is an artificial neural network based on a breakthrough of the wavelet analysis. WNN is a novel hierarchical and multi-resolution artificial neural network model based on wavelet analysis theory and wavelet transform. The S-type activation function of the hidden node in the neural network is replaced with the wavelet function. The corresponding weight from the input layer to the hidden layer, and the threshold value of the hidden layer are replaced with scale expansion and time shift factors of wavelet function, respectively.

The determination of the number of hidden layer nodes is a key factor influencing the accuracy of the WNN prediction model. Therefore, the number of hidden layer nodes is determined under the condition of meeting the model accuracy, and the compactness of the model structure is ensured to avoid redundancy. In the present study, the number of hidden layer nodes was set to five, and the model was trained with five, eight, 10, 12, 16, and 20 hidden layer nodes. The training error, test error, and model training time are presented in Table 3. Prediction MRE is considered minimum when the number of hidden nodes is 10. Therefore, the number of hidden nodes was set to 10, the learning rate was 0.01, the number of iterations was 1000, and the maximum allowable error was 0.001. WNN was created in MATLAB R2019b software (MathWorks, Inc. Natick, Massachusetts, USA).

After classifying, processing, and filtering the data based on the relevant theory of WNN, the parameters were initialized and the training data were input. In addition, the error value was calculated and the

parameters were corrected. A WNN prediction model for petiole NO_3^--N content in cotton under drip irrigation was developed based on spectral indices through repeated training and iterations. The prediction accuracy of the model was continuously enhanced and errors were reduced. The specific flow chart of developing WNN is illustrated in Fig 2.

RF [42] is an algorithm that integrates multiple trees through ensemble learning and its basic unit is a decision tree. RF is widely used in high-dimensional data classification and regression. The RF algorithm was developed using in MATLAB R2019b software (MathWorks, Inc. Natick, Massachusetts, USA). The number of classification trees in RF algorithm was 1070.

RBF [42] can fit continuous nonlinear functions, and its hidden layer adopts RBF, which will responds to input signals locally. In the present study, RBF neural network was developed using MATLAB R2019b software (MathWorks, Inc. Natick, Massachusetts, USA), and the variance parameter of RBF kernel function was set to 0.3.

BP neural network [42] is a learning algorithm of feedback networks, which reflects the input−output relationship of samples, and has strong nonlinear fuzzy approximation ability. In the present study, a BP neural network was developed in MATLAB R2019b software (MathWorks, Inc. Natick, Massachusetts, USA). The BP neural network adopts a three layer structure, with 10 hidden layer nodes, 1000 iterations, and 0.01 learning rate.

Results

Relationship between petiole NO_3^--N content and 'trilateral parameters'

The correlation analyses results of NO_3^--N content and 'trilateral parameters' of cotton petioles under drip irrigation are presented in Table 4. The correlation between NO_3^--N content in petioles and blue edge parameters was stronger than those of red edge and yellow edge parameters, although the correlations reached extremely significant levels; a negative correlation was observed among red edge amplitude (Dr), red edge area (SDr) , yellow edge amplitude (Dy) , and yellow edge area (SDy), while a positive correlation was observed between blue edge amplitude (Db) and blue edge area (SDb). The correlation coefficients of Db and SDb were 0.90.

Regression analyses between NO_3^--N content in petioles and 'trilateral parameters' during the key growth period of cotton under drip irrigation presented Table 5. The regression equation of blue edge parameters and petiole NO_3^--N content R^2 was higher and RMSE was lower than those of red edge and yellow edge parameters. Polynomial regression equation of Db exhibited the highest coefficient of determination (R^2 = 0.89), and the RMSE value of Db linear regression equation was the lowest (1.04 g/L). Based on the linear regression equations of blue edge and red edge parameters, R^2 value of Db in blue edge parameters increased by 25.0% when compared with Dr in red edge parameters, while the R^2 value of SDb in blue edge parameters is increased by 55.8% compared with SDr in red edge parameters.

Relationship between NO_3^--N content in petioles and vegetation indices

The correlation analyses results between NO_3^--N content in petioles under drip irrigation and six sets of original spectral reflectance data, the correlation analysis shows that, as shown in Table 6, revealed a significant negative correlation between vegetation index red edge (RD) and NO_3^--N content in petioles, with a correlation coefficient of -0.81, followed by near infrared ratio spectral index (NIR), with a correlation coefficient of -0.79, and other vegetation indices that reached significant correlation levels (Table 6). Correlation analyses of NO_3^--N content in cotton petioles under drip irrigation and the vegetation indices developed based on the first six sets of derivative spectral data revealed that ND705 had a significant negative correlation with NO_3^--N content in petioles, and the correlation coefficient was -0.90, followed by red edge model index ($CI_{red-edge}$), with a correlation coefficient of -0.89 (Table 6). The correlation coefficients of ND705 and NO_3^--N content in petioles significantly increased by 18.4% and 20.3%, respectively except for NIR based on ND705 and $CI_{red-edge}$.

Regression analyses between the NO_3^--N content in petioles and six vegetation indices during the key growth period of cotton under drip irrigation revealed that R^2 values the first derivative vegetation indices, RD, $CI_{red-edge}$, normalized difference red edge index (NDRE), and normalized difference spectral index (ND705) were generally higher than those of the original vegetation index, and the RMSE values were generally lower than those of original vegetation indices. The R^2 values of NIR and Red edge ratio spectral index (RI-1dB) were higher than those of the first derivative vegetation indices, and RMSE values were lower than those of the first derivative vegetation indices. Among the three regression models, the R^2 value of the polynomial regression equation for the first derivative vegetation index, ND705 was the highest (R^2 = 0.83), and the linear regression equation of the first derivative vegetation index, $CI_{red- edge}$ had the lowest RMSE (0.92 g/L). In summary, the first derivative vegetation index, ND705 and $CI_{red-edge}$ exhibited higher prediction ability. The R^2 value of the polynomial regression equation between ND705 and petiole NO_3^--N content was 53.4% higher than that of ND705, and RMSE value of the linear regression equation of the first derivative vegetation index and petiole NO_3^--N content was 45.6% lower than that of the original vegetation index, $CI_{red-edge}$.

Development and verification of estimation model using WNN

In the present study, two stable and representative first derivative vegetation indices (ND705, $CI_{red-edge}$) and Db and SDb (blue edge parameters) were used to develop petiole NO_3^--N content estimation model WNN. The simulated and measured values were fitted and analyzed using independent validation test data. The results are presented in Table 8. The R^2, RMSE, and MAE values of the WNN estimation model based on the first derivative vegetation indices were 0.81, 0.91g/L, and 0.73g/L, respectively, while the R^2, RMSE, and MAE values of the validation model were 0.82, 0.87 g/L, and 0.68g/L, respectively. The R^2, RMSE, and MAE values of the WNN estimation model based on blue edge parameters were 0.88, 0.74 g/L

and 0.58 g/L, respectively. The R^2, RMSE, and MAE values of the validation model based on blue edge parameters were 0.88, 0.65 g/L, and 0.47g/L, respectively. R^2 value of WNN based on blue edge parameters increased by 8.6%, whereas RMSE and MAE values reduced by 18.7% and 20.5%, respectively, when Compared with the estimation model based on vegetation indices. R^2 value of the validation model based on blue edge parameters increased by 7.3%, whereas RMSE and MAE values reduced by 25.2% and 30.9%, respectively, when Compared with the estimation model based on vegetation indices. Generally, R^2 value of the validation model was higher than that of the estimation model, while RMSE and MAE values were lower than those of the estimation model, suggesting that the validation model is stable.

Comparative analysis of model validation with other mainstream methods

Develop the estimation model of NO_3-N content in petioles based on WNN, RF, RBF and BP (Table 9). The R^2, RMSE and MAE values of the WNN validation model based on the first derivative vegetation index were 0.82, 0.87 g/L, and 0.68 g/L, respectively; R^2, RMSE, and MAE values of the RF verification model were 0.82, 0.92 g/L, and 0.76 g/L, respectively; R^2, RMSE, and MAE values of the RBF estimation model were 0.82, 0.88 g/L, and 0.72 g/L, respectively; R^2, RMSE and MAE values of the BP estimation model were 0.74, 1.02 g/L, and 0.81 g/L, respectively. In addition, the R^2 values of WNN, RF, and RBF were all 0.82; however, the RMSE and MAE values of WNN are 5.4% and 10.5% lower than those of RF, 1.0% and 5.6% lower than those of RBF, and 17.2% and 16.0% lower than those of BP.

The R^2, RMSE, and MAE values of the WNN validation model based on blue edge parameters were 0.88, 0.65 g/L, and 0.47 g/L, respectively; R^2, RMSE, and MAE values of the RF verification model were 0.82, 0.79 g/L, and 0.60 g/L, respectively; the R^2, RMSE, and MAE values of the RBF estimation model were 0.81, 0.80 g/L, and 0.61 g/L, respectively; R^2, RMSE and MAE values of the BP estimation model were 0.77, 0.89 g/L, and 0.65 g/L, respectively. Furthermore, compared with RF, the R^2 value of WNN increased by 7.3%, whereas RMSE and MAE values decreased by 17.7% and 21.7%, respectively; compared with RBF, the R^2 of WNN increased by 8.6%, whereas RMSE and MAE values decreased by 18.8% and 23.0%, respectively; compared with BP, the R^2 of WNN increased by 14.3%, whereas RMSE and MAE values decreased by 27.0% and 27.7%, respectively.

The R^2 value of the WNN model based on blue edge parameters is increased by 7.3%, RMSE and MAE values reduced by 25.2% and 30.9%, respectively when compared with the model based on vegetation indices.

Discussion

Feasibility of remote sensing monitoring NO_3^--N content in cotton petioles under drip irrigation

Timely and accurate monitoring of N nutrition in crops is the key to accurate application of N fertilizer [43]. The rapid development of remote sensing technology presents a potential novel method for

monitoring crop nutrition [44]. Local and international researchers have used the technology to monitor plant N content and N accumulation, although research NO_3^--N in cotton petioles under drip irrigation is scarce [45]. Monitoring of petiole NO_3^--N content is a widely used approach in crop nutrition diagnosis and topdressing recommendation [44]. In the present study, the correlations among six 'trilateral parameters' and six vegetation indices, and NO_3^--N content in cotton petioles under drip irrigation was analyzed and the results revealed that large proportion of the spectral index was strongly correlated with NO_3^--N in petioles, suggesting estimation NO_3^--N content in cotton petioles under drip irrigation using spectral indices is feasible.

Potential of blue edge parameters the estimation NO_3^--N content in petioles

'Trilateral parameters', especially the red edge parameters can effectively reflect the characteristics of crop N status [46]. Previous studies on wheat, rice, and other crops have developed N content estimation models based on red edge parameters and achieved satisfactory results [47, 48]. However, the present established that the correlation between blue edge parameters and petiole NO_3^--N content was strong, and that the traditional regression model of blue edge parameters and petiole NO_3^--N content was superior to the red edge and yellow edge parameters. The estimation and validation models based on blue edge parameters and WNN exhibited superior capacity to the vegetation index model based on the red edge band. The observation is relatively inconsistent with the findings of most previous studies, which focused on the correlation between red edge parameters and crop N. Studies have revealed that blue edge is sensitive to crop N. Li et al. [49] determined the N nutrition in winter wheat by conducting hyperspectral analyses, and established that blue–violet light was sensitive to N. Stroppiana et al. [50] demonstrated that blue light was the ideal wave segment for N estimation in rice. The results obtained in the present study could be due to the variations in crop canopy structure and biomass, or the unique climatic conditions in Xinjiang, drip irrigation fertilization methods, and other factors.

Most of the researchers are more interested in the red edge parameters and pay less attention to the blue edge parameters, which cover wavelengths between 490 and 530 nm, when selecting spectral characteristic parameters. Therefore, blue edge parameters should be taken into consideration when determining N nutrition based on spectral data. The present study further demonstrated the potential of blue edge parameters in the estimation of N content in crops.

Application of neural networks in remote sensing monitoring

The R^2 value of the WNN estimation and verification models were relatively high, while RMSE and MAE values were relatively low, suggesting that the stability of the model is high, and the estimation capacity of the model is superior. Combined WNN maintains the advantages of artificial neural networks and wavelet analysis, which accelerates network convergence in turn, preventing the algorithm from falling into local optimum and occasionally makes local analysis more frequent [51, 52]. The RBF neural network algorithm confers the advantages of rapid training and convergence speed, strong input–output

mapping ability, and strong generalization ability when compared with BP neural network algorithm. Furthermore, the results of the present study revealed that the estimation model based on the RBF neural network is superior BP neural network model [53].

Numerous studies have revealed that neural networks exhibit a great potential in learning and developing nonlinear complex relationship models, and they exhibit high tolerance for input objects . Neural networks can simulate heteroscedasticity better and have the ability to learn hidden relations in data without imposing any fixed relations in the data [53, 54].

The present study was conducted in experimental plots and the method used to determine NO_3^--N content in petioles caused considerable damage to plant tissues. Therefore, the number of samples analyzed was limited, which could influence the accuracy of modeling. The sampling frequency from bud stage to flowering and boll stage should be increased, and more data should be acquired to further improve the modeling capacity of the estimation model.

Comparison between WNN and RF

Most of the previous studies on crop physiological parameter estimation have demonstrated that the RF algorithm exhibits high accuracy and estimation ability, and confers the advantages of strong stability and high efficiency when compared with other modeling methods. Loozen et al. [55] used RF technology estimate the N content of a European forest canopy, which exhibited superior accuracy (R^2 = 0.62, RMSE = 0.18). To establish an efficient method for estimating winter wheat biomass, Yue et al. [56] used RF algorithm to develop a regression model of winter wheat biomass by combining spectrum, radar backscattering, vegetation index, and radar vegetation index, and the results revealed the potential application of stochastic forest algorithm in remote sensing to estimate winter wheat biomass. The RF regression algorithm has been demonstrated to result in over fitting phenomenon and high test errors when compared with neural network algorithm [57]. RMSE and MAE values of WNN and RBF models based on the vegetation indices are lower than those of the RF model during model validation (Fig. 3). The R^2 value of WNN based on blue edge parameters was higher than that of the RF model, and RMSE and MAE values were lower than those of the RF model (Fig. 4), which is consistent with previous findings that the RF method exhibited weak prediction ability [58].

Conclusions

The present study analyzed and compared the performance of 'trilateral parameters' and vegetation indices in estimating NO_3^--N content in cotton petioles under drip irrigation, in addition to determining an effective method to estimate NO_3^--N content in cotton petioles under drip irrigation using blue edge parameters and WNN. The results revealed the capacity to NO_3^--N content in cotton petioles based on blue edge parameters was significantly improved when compared with red edge parameters and common vegetation indices. The validation model based on blue edge parameters and WNN exhibited the highest coefficient (R^2 = 0.88), lowest root mean square error (RMSE = 0.65 g/L) and lowest mean absolute error

(MAE = 0.47 g/L). Our study demonstrates the potential application of blue edge parameters and WNN in estimating NO_3^--N content in cotton petioles under drip irrigation.

Declarations

Author details

[1] School of Agriculture, Shihezi University, Shihezi 832003, P.R.China

[2] National and local joint engineering research center of information management and Application Technology for modern agricultural production (XPCC), Shihezi 832003, P.R.China

Acknowledgements

Authors' contributions

ZD contributed to the conceptualization, Methodology, software, data curation, writing - original draft preparation, writing- reviewing and editing. YL and FM contributed to the writing - reviewing and editing, supervision, project administration, funding acquisition. BC, MW, ML, XL, XF, SW contributed to the investigation, data curation, resources.

Competing interests

The authors declare that they have no known competing financial interests or personal relationships that could have appeared to influence the work reported in this paper.

Availability of data and materials

The remotely sensed and field sampling data used in this study is available from the corresponding author on reasonable request.

Consent for publication

All authors agreed to publish this manuscript.

Ethics approval and consent to participate

All authors read and approved the manuscript.

Funding

References

1. Rochester IJ, Constable GA. Nitrogen-fertiliser application effects on cotton lint percentage, seed size, and seed oil and protein concentrations. Crop Pasture Science. 2020;71:831–6.

2. Li YY, Gao XP, Tenuta M, Gui DW, Li XY, Xue W, Zeng FJ. Enhanced efficiency nitrogen fertilizers were not effective in reducing N_2O emissions from a drip-irrigated cotton field in arid region of Northwestern China. Science of The Total Environment. 2020;748:p.141543.

3. Yang XY, Geng JB, Huo XQ, Lei ST, Lang Y, Li H, Liu QJ. Effects of different nitrogen fertilizer types and rates on cotton leaf senescence, Yield and Soil Inorganic Nitrogen. 2020.

4. Echer FR, Cordeiro CFD, de la Torre EDR. The effects of nitrogen, phosphorus, and potassium levels on the yield and fiber quality of cotton cultivars. J Plant Nutr. 2020;43:921–32.

5. Wei CZ, Zhang FS, Zhu HM, Hou ZA, Guo GS, Bao BY. Study on nitrogen nutrition diagnosis and topdressing recommendation of cotton in Xinjiang. Chinese Journal of Agricultural Sciences, 2002;1500–1505.

6. Wang LS, Khan Aziz, Yuan Y, Wu YY, Shah AN, Tung S, Yang GZ. Effects of sowing date and density on NO_3^--N content in cotton petioles and roots. Acta cotton Sinica. 2016;28:574–83.

7. Darnell RL, Stutte GW, Sager JC. Nitrate concentration effects on NO_3^--N uptake and reduction, growth, and fruit yield in strawberry. J Am Soc Hortic Sci. 2001;126:560.

8. Brito DDMCD, Santos CD, Goncalves FV, et al. Effects of nitrate supply on plant growth, nitrogen, phosphorus and potassium accumulation, and nitrate reductase activity in crambe. J Plant Nutr. 2013;36:275–83.

9. Wu SH, Liu JF, Cheng JY. Study on nitrate nitrogen in cotton petioles as a diagnostic index of nitrogen nutrition. Hubei Agricultural Science. 1987;19–22.

10. Carlson RM, Cabrera RI, Paul JL, Quick J, Evans RY. Rapid direct determination of ammonium and nitrate in soil and plant tissue extracts. Communications in Soil Science Plant Analysis. 1990;21:1519–29.

11. Singh D, Singh K, Hundal HS, Sekhon KS. Diagnosis and recommendation integrated system (dris) for evaluating nutrient status of cotton (gossipium hirsutum). J Plant Nutr. 2006;29:113–25.

12. Qu P, Xu WH, Crop Nutrition and Computer Vision Technology. Wireless Personal Communications. 2020.

13. Rosolem CA, van Mellis V. Monitoring nitrogen nutrition in cotton. Revista Brasileira de Ciência do Solo. 2020;34:1601–7.

14. Woodson WR, Boodley JW. Petiole nitrate concentrationas an indicator of geranium nitrogen status. Commun Soil Sci Plant Anal. 1983;14:363–71.

15. Keisling TC, Mascagni NJ, Maples RL, Thompson KC. Using cotton petiole nitrate nitrogen concentration for prediction of cotton nitrogen nutritional status of a clayey soil. J Plant Nutr. 1995;18:35–45.

16. Saranga Y, Landa A, Shekel Y. Near-Infrared Analysis of Cotton Leaves as a Guide for Nitrogen Fertilization. Agronomy Journal. 1998;90.

17. Boggs JL, Tsegaye TD, Coleman TL. Relationship Between Hyperspectral Reflectance, Soil Nitrate-Nitrogen, Cotton Leaf Chlorophyll, and Cotton Yield: A Step Toward Precision Agriculture. Journal of Sustainable Agriculture. 2003;22:5–16.

18. Banerjee BP, Spangenberg G, Kant S. Fusion of Spectral and Structural Information from Aerial Images for Improved Biomass Estimation. Remote Sensing. 2020;12.

19. Liu N, Zhao R, Qiao L. Growth Stages Classification of Potato Crop Based on Analysis of Spectral Response and Variables Optimization. Sensors. 2020;20:3995.

20. Chang CY, Zhou R, Kira O. An Unmanned Aerial System (UAS) for concurrent measurements of solar-induced chlorophyll fluorescence and hyperspectral reflectance toward improving crop monitoring. Agric For Meteorol. 2020;294:108145.

21. Wang W, Yao X, Tian YC. Common spectral bands and optimum vegetation indices for monitoring leaf nitrogen accumulation in rice and wheat. Journal of Integrative Agriculture. 2012;11:2001–12.

22. Liu S, Li L, Fan H. Real-time and multi-stage recommendations for nitrogen fertilizer topdressing rates in winter oilseed rape based on canopy hyperspectral data. Ind Crops Prod. 2020;154:112699.

23. Yadav VP, Prasad R, Bala R, Srivastava PK. Assessment of red-edge vegetation descriptors in a modified water cloud model for forward modelling using Sentinel–1A and Sentinel–2 satellite data. Int J Remote Sens. 2021;42:794–804.

24. Dalen M, Tubana B, Kanke Y. Relationship of red and red-edge reflectance-based vegetation indices with stalk and fiber yield of energy cane harvested at different dates. Arch Agron Soil Sci. 2019;66:1888–907.

25. Hansen PM, Schjoerring JK. Reflectance measurement of canopy biomass and nitrogen status in wheat crops using normalized difference vegetation indices and partial least squares regression. Remote Sens Environ. 2003;86:542–53.

26. Railyan VY, Korobov RM. Red edge structure of canopy reflectance spectra of triticale. Remote Sens Environ. 1993;46:173–82.

27. María A, Gilabert. Soledad Gandía, Joaquín Meliá. Analyses of spectral-biophysical relationships for a corn canopy. Remote Sens Environ. 1996;55:11–20.

28. Feng S, Xu TY, Yu FH, Chen CL, Yang X, Wang NY. Research of Method for Inverting Nitrogen Content in Canopy Leaves of Japonica Rice in Northeastern China Based on Hyperspectral Remote Sensing of Unmanned Aerial Vehicle. Spectroscopy Spectral Analysis. 2019;39:3281–7.

29. Xiu LN, Zhang H, Guo QZ, Wang ZH, Liu XN, Estimating nitrogen content of corn based on wavelet energy coefficient and BP neural network. 2015 2ND International Conference On Information Science and Control Engineering. 2015;212–216.

30. Anshuka A, Buzacott AJV, Vervoort RW, van Ogtrop FF. Developing Drought Index Based Forecasts for Tropical Climates using Wavelet Neural Network: An Application in Fiji. Theoretical and Applied Climatology. 2020.

31. Lee Minjae K, Hyemi. Kim Hee-Joung. Sparse-view CT reconstruction based on multi-level wavelet convolution neural network. Physica Med. 2020;80:352–62.

32. Jouila A, Nouri K. An Adaptive Robust Nonsingular Fast Terminal Sliding Mode Controller Based on Wavelet Neural Network for a 2-DOF Robotic Arm. J Franklin Inst. 2020;357:13259–82.

33. Ghoddusi H, Creamer GG, Rafizadeh N. Machine learning in energy economics and finance: A review. Energy Econ. 2019;81:709–27.

34. Horler DNH, Dockray M, Barber J. The red edge of plant leaf reflectance. Int J Remote Sens. 1983;4:273–88.

35. Wang XP, Zhang F, Kung HT, Yu HY. Spectral response characteristics and identification of typical plant species in Ebinur lake wetland national nature reserve (ELWNNR) under a water and salinity gradient. Ecol Ind. 2017;81:222–34.

36. Vogelmann JE, Rock BN, Moss DM. Red edge spectral measurements from sugar maple leaves. International Journal of Remote Sensing. 1993;14:1563–75.

37. Gitelson AA, Vina A, Ciganda V. Remote estimation of canopy chlorophyll content in crops. Geophysical Research Letters. 2005;32.

38. Barnes EM, Clarke TR, Richards SE. Coincident detection of crop water stress, nitrogen status and canopy density using ground based multispectral data. Bloomington, MN, USA. Proceedings of the Fifth International Conference on Precision Agriculture. 2000;1619.

39. Gitelson A, Merzlyak MN. Spectral Reflectance Changes Associated with Autumn Senescence of Aesculus hippocastanum L. and Acer platanoides L. Leaves. Spectral Features and Relation to Chlorophyll Estimation. J Plant Physiol. 1994;143:286–92.

40. Mistele B, Schmidhalter U. Tractor-Based Quadrilateral Spectral Reflectance Measurements to Detect Biomass and Total Aerial Nitrogen in Winter Wheat. Agron J. 2010;102:499–506.

41. Gupta R, Vijayan D, Prasad T. Comparative analysis of red-edge hyperspectral indices. Adv Space Res. 2003;32:2217–22.

42. Zhou ZH. machine learning. Beijing: Tsinghua university press; 2015.

43. Kodur S, Shrestha UB, Maraseni TN. Environmental and economic impacts and trade-offs from simultaneous management of soil constraints, nitrogen and water. J Clean Prod. 2019;222:960–70.

44. Wu JD, Wang D, Rosen CJ. Comparison of petiole nitrate concentrations, SPAD chlorophyll readings, and Quick Bird satellite imagery in detecting nitrogen status of potato canopies. Field Crops Research. 2015;101:96–103.

45. Lu J, Miao Y, Shi W. Developing a Proximal Active Canopy Sensor-based Precision Nitrogen Management Strategy for High-Yielding Rice. Remote Sensing. 2020;12:1440.

46. Wheeler KI, Levia DF, Vargas R. Visible and near-infrared hyperspectral indices explain more variation in lower-crown leaf nitrogen concentrations in autumn than in summer. Oecologia. 2020;192:13–27.

47. Harika N. Dishant, et al. Developing a new Crop Circle active canopy sensor-based precision nitrogen management strategy for winter wheat in North China Plain. Remote Sensing. 2020;9.

48. Jiang J, Zhang ZY, Cao Q, Liang Y, Krienke B, Tian YC, Zhu Y, Cao WX, Liu XJ. Use of an Active Canopy Sensor Mounted on an Unmanned Aerial Vehicle to Monitor the Growth and Nitrogen Status of Winter Wheat. Remote Sensing. 2020;12.

49. Li F, Miao Y, Hennig SD. Evaluating hyperspectral vegetation indices for estimating nitrogen concentration of winter wheat at different growth stages. Precision Agric. 2010;11:335–57.

50. Stroppiana D, Boschetti M, Brivio PA. Plant nitrogen concentration in paddy rice from field canopy hyperspectral radiometry. Field Crops Research. 2009;111:119–29.

51. Ghamariadyan M, Imteaz MA. A wavelet artificial neural network method for medium term rainfall prediction in Queensland (Australia) and the comparisons with conventional methods. International Journal of Climatology. 2020.

52. Dong YH, Fu ZT, Peng YQ, Zheng YJ, Yan HJ, Li XX. Precision fertilization method of field crops based on the Wavelet-BP neural network in China. Journal of Cleaner Production. 2019;246.

53. Basheer IA, Hajmeer M. Artificial neural networks: fundamentals, computing, design, and application. J Microbiol Methods. 2000;43:3–31.

54. Taghadomi-Saberi S, Masoumi AA, Sadeghi M, Zekri M. Integration of wavelet network and image processing for determination of total pigments in bitter orange (Citrus aurantium L.) peel during ripening. Journal of Food Process Engineering. 2019;42:e13120.1–e13120.8..

55. Loozen Y, Rebel KT, de Jong SM, Lu M, Ollinger SV, Wassen MJ, Karssenberg D. Mapping canopy nitrogen in European forests using remote sensing and environmental variables with the random forests method. Remote Sensing of Environment. 2020;247.

56. Yue Jibo, Yang GJ, Feng HK. Comparison of remote sensing estimation models for winter wheat biomass based on Stochastic Forest algorithm. Agricultrual Engineering. 2016;32:175–82.

57. Breiman Leo. Mach Learn. 2001;45:5–32.

58. Han ZY, Zhu XC, Fang XY, Wang ZY, Wang L, Zhao GX, Jiang YM. Hyperspectral Estimation of Lai in Apple Crown Based on SVM and RF. Spectroscopy Spectral Analysis. 2016;36:800–5.

Tables

Table 1 LAQUA twin NO$_3$-N instrument profile

Instruments name	LAQUA twin NO$_3^-$
Measuring principles	Ion electrode
Volume of samples required	0.3-2.0 mL
Scope of measurement	2-9900mg/L

Table 2 Calculation methods and reflectance of spectral indices

Spectral index		Abbreviation	Formula	Reference
Trilateral parameters	Red edge amplitude	Dr	Maximum first derivative within 680-760	[34]
	Red edge area	SDr	Sum of first derivative values in red edge	[34]
	Yellow edge amplitude	Dy	Maximum first derivative within 560-640	[35]
	Yellow edge area	SDy	Sum of first derivative values in yellow edge	[35]
	Blue edge amplitude	Db	Maximum first derivative within 490-530	[35]
	Blue edge area	SDb	Sum of first derivative values in blue edge	[35]
Vegetation index	Red edge ratio spectral index	RD	R_{740}/R_{720}	[36]
	Red edge model index	CI$_{red-edge}$	$(R_{780}/R_{710})-1$	[37]
	Normalized difference red edge index	NDRE	$(R_{790}-R_{720})/(R_{790}+R_{720})$	[38]
	Normalized difference spectral index	ND705	$(R_{750}-R_{705})/(R_{750}+R_{705})$	[39]
	Near infrared ratio spectral index	NIR	R_{780}/R_{740}	[40]
	Red edge ratio spectral index	RI-1dB	R_{735}/R_{720}	[41]

Table 3 Influence of the number of nodes in different hidden layers on network prediction error

Learning rate	Number of iterations	Maximum allowable error	Number of hidden layer nodes	MRE%
0.01	1000	0.001	5	7.14
0.01	1000	0.001	8	5.86
0.01	1000	0.001	10	5.82
0.01	1000	0.001	12	6.92
0.01	1000	0.001	16	6.35
0.01	1000	0.001	20	5.92

Table 4 Correlation coefficient between NO_3^--N content of petioles and 'trilateral parameters'

Trilateral parameters	Correlation coefficients
Dr	-0.80**
SDr	-0.72**
Dy	-0.85**
SDy	-0.59**
Db	0.90**
SDb	0.90**

Table 5 Quantitative relationship between 'trilateral parameters' and NO_3^--N content in petioles

Trilateral parameters	Functional model	Regression equation	R^2	RMSE (g/L)
Dr	Linear	y = -1E+06x + 21084	0.64	1.40
	Exponential	$y = 59355e^{-160.9x}$	0.61	1.45
	Quadratic	$y = -2E+08x^2 + 6E+06x - 23990$	0.67	2.93
SDr	Linear	y = -12321x + 13673	0.52	2.28
	Exponential	$y = 18355e^{-1.876x}$	0.47	2.59
	Quadratic	$y = -58926x^2 + 48072x - 895.38$	0.60	2.53
Dy	Linear	y = -1E+08x + 1114.1	0.72	1.08
	Exponential	$y = 2691.4e^{-17931x}$	0.67	1.82
	Quadratic	$y = -4E+12x^2 - 5E+08x - 9212.4$	0.84	2.73
SDy	Linear	y = -193244x - 1139.4	0.73	2.91
	Exponential	$y = 1924.3e^{-29.42x}$	0.67	2.54
	Quadratic	$y = -8E+06x^2 - 905730x - 16273$	0.79	2.51
Db	Linear	y = 4E+06x - 836.47	0.80	1.04
	Exponential	$y = 2036.5e^{619.48x}$	0.72	1.50
	Quadratic	$y = -3E+09x^2 + 2E+07x - 14359$	0.89	1.64
SDb	Linear	y = 498071x - 9405.9	0.81	1.45
	Exponential	$y = 492.37e^{78.986x}$	0.80	1.53
	Quadratic	$y = 9E+06x^2 - 84605x - 199.84$	0.82	1.98

Table 6 Correlation coefficient between NO_3^--N content of petioles and vegetation indices

Type of reflectivity	Vegetation indices	Correlation coefficients
First derivative	RD	-0.85**
	$CI_{red-edge}$	-0.89**
	NDRE	-0.80**
	ND705	-0.90**
	NIR	-0.62**
	RI-1dB	-0.72**
Original	RD	-0.81**
	$CI_{red-edge}$	-0.74**
	NDRE	-0.77**
	ND705	-0.76**
	NIR	-0.79**
	RI-1dB	-0.77**

Table 7 Quantitative relationship between spectral indices and NO_3^--N content

Type of reflectivity	Vegetation indices	Functional model	Regression equation	R^2	RMSE (g/L)
First derivative	RD	Linear	$y = -8116.9x + 13150$	0.71	1.77
		Exponential	$y = 17860e^{-1.306x}$	0.73	2.01
		Quadratic	$y = 3178.2x^2 - 13332x + 15120$	0.72	1.88
	$CI_{red-edge}$	Linear	$y = -76288x - 66089$	0.80	0.92
		Exponential	$y = 0.067e^{-12.01x}$	0.78	0.98
		Quadratic	$y = -169389x^2 - 400646x - 221261$	0.80	0.93
	NDRE	Linear	$y = -27424x - 18368$	0.63	1.14
		Exponential	$y = 147.75e^{-4.115x}$	0.56	1.23
		Quadratic	$y = 126872x^2 + 207536x + 89944$	0.67	1.18
	ND705	Linear	$y = -18527x + 3265$	0.82	1.52
		Exponential	$y = 3707.4e^{-2.893x}$	0.78	1.35
		Quadratic	$y = -29935x^2 - 30687x + 2342.8$	0.83	1.69
	NIR	Linear	$y = -85125x + 10408$	0.39	1.45
		Exponential	$y = 11137e^{-12.9x}$	0.35	1.55
		Quadratic	$y = -2E+06x^2 + 47910x + 8644.1$	0.44	1.44
	RI-1dB	Linear	$y = -19373x + 22583$	0.52	2.37
		Exponential	$y = 78853e^{-3.076x}$	0.52	2.91
		Quadratic	$y = 126872x^2 + 207536x + 89944$	0.59	2.83
	RD	Linear	$y = -8564.7x + 25826$	0.65	1.50
		Exponential	$y = 131902e^{-1.36x}$	0.65	1.57

				R^2	RMSE
Original		Quadratic	$y = -10788x^2 + 39287x - 26804$	0.67	1.47
	$CI_{red-edge}$	Linear	$y = -3415.6x + 14222$	0.54	1.69
		Exponential	$y = 19774e^{-0.516x}$	0.49	1.81
		Quadratic	$y = -357.75x^2 - 1914.2x + 12720$	0.54	1.67
	NDRE	Linear	$y = -28351x + 17684$	0.59	1.70
		Exponential	$y = 34790e^{-4.394x}$	0.56	1.81
		Quadratic	$y = -202849x^2 + 124311x - 10381$	0.63	1.60
	ND705	Linear	$y = -2745.6x + 16233$	0.58	2.38
		Exponential	$y = 29232e^{-0.441x}$	0.59	2.41
		Quadratic	$y = -35.761x^2 - 2493x + 15800$	0.58	2.34
	NIR	Linear	$y = -28744x + 38765$	0.62	1.66
		Exponential	$y = 946939e^{-4.488x}$	0.60	1.81
		Quadratic	$y = -180524x^2 + 369826x - 180634$	0.66	1.53
	RI-1dB	Linear	$y = -10960x + 28560$	0.59	1.58
		Exponential	$y = 199238e^{-1.729x}$	0.58	1.67
		Quadratic	$y = -26273x^2 + 92468x - 72663$	0.64	1.52

Table 8 Modeling and validation of NO_3^--N content in petioles by Wavelet Neural Network

Spectral index type	Modeling				Validation			
	Number of samples	R^2	RSME (g/L)	MAE (g/L)	Number of samples	R^2	RSME (g/L)	MAE (g/L)
Vegetation indices	60	0.81	0.91	0.73	60	0.82	0.87	0.68
Blue edge parameters	60	0.88	0.74	0.58	60	0.88	0.65	0.47

Table 9 Validation between predicted and measured of NO$_3^-$-N content in petioles based on different methods

Methods	Blue edge parameters				Vegetation indices			
	Number of samples	R^2	RSME (g/L)	MAE (g/L)	Number of samples	R^2	RSME (g/L)	MAE (g/L)
WNN	60	0.88	0.65	0.47	60	0.82	0.87	0.68
RF	60	0.82	0.79	0.60	60	0.82	0.92	0.76
RBF	60	0.81	0.80	0.61	60	0.82	0.88	0.72
BP	60	0.77	0.89	0.65	60	0.74	1.02	0.81

Figures
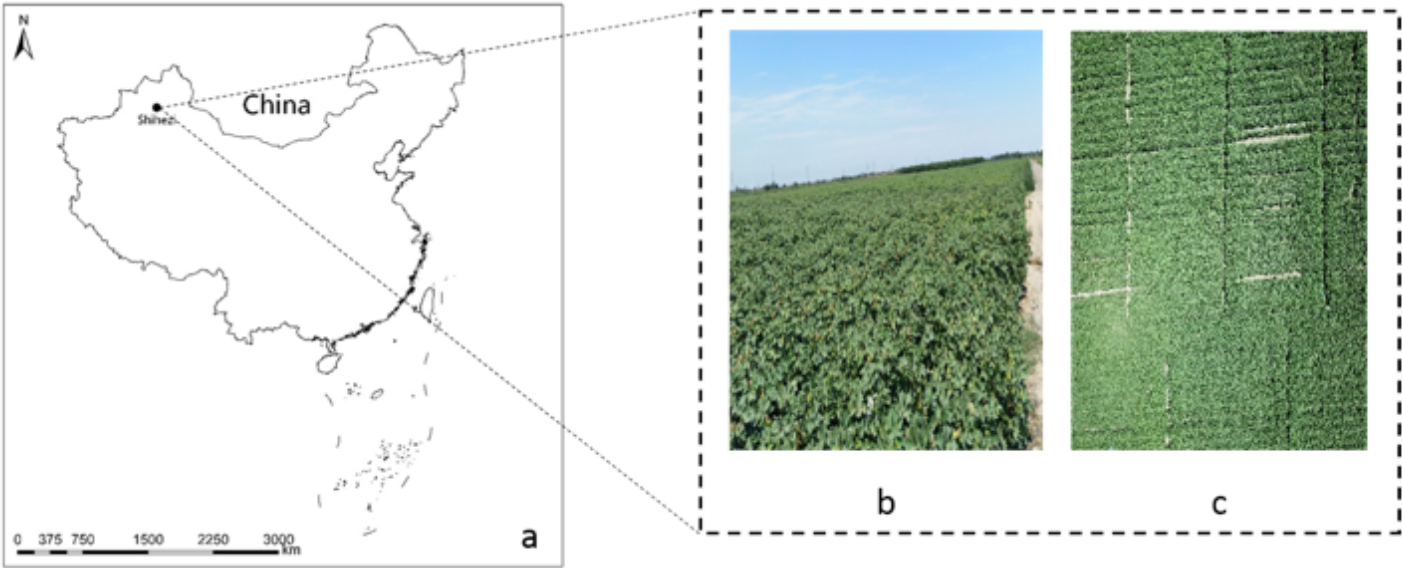
Figure 1

Study area location. a location of the study area; b field experiment; c high yield verification cotton field photographed by UAV. Note: The designations employed and the presentation of the material on this map do not imply the expression of any opinion whatsoever on the part of Research Square concerning the legal status of any country, territory, city or area or of its authorities, or concerning the delimitation of its frontiers or boundaries. This map has been provided by the authors.
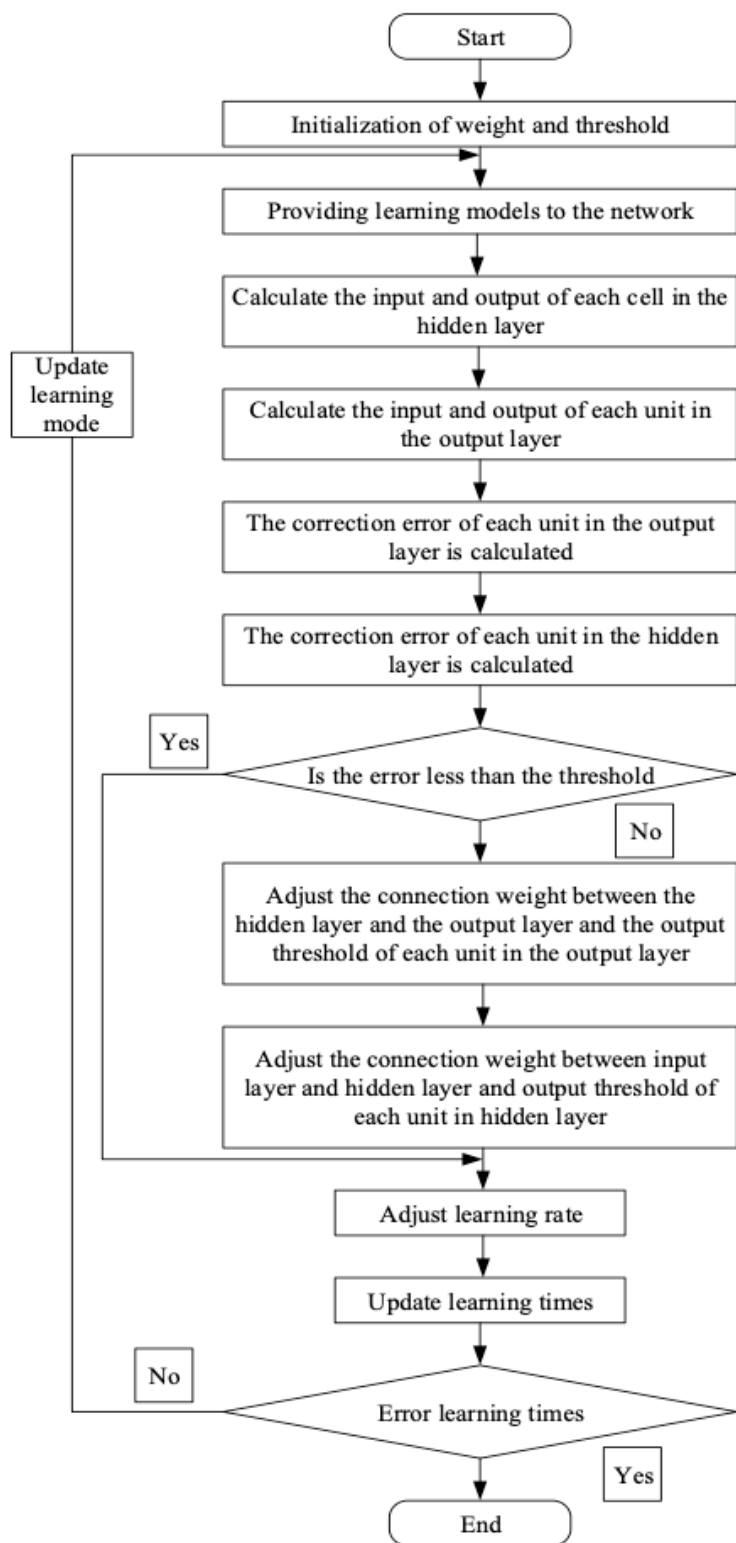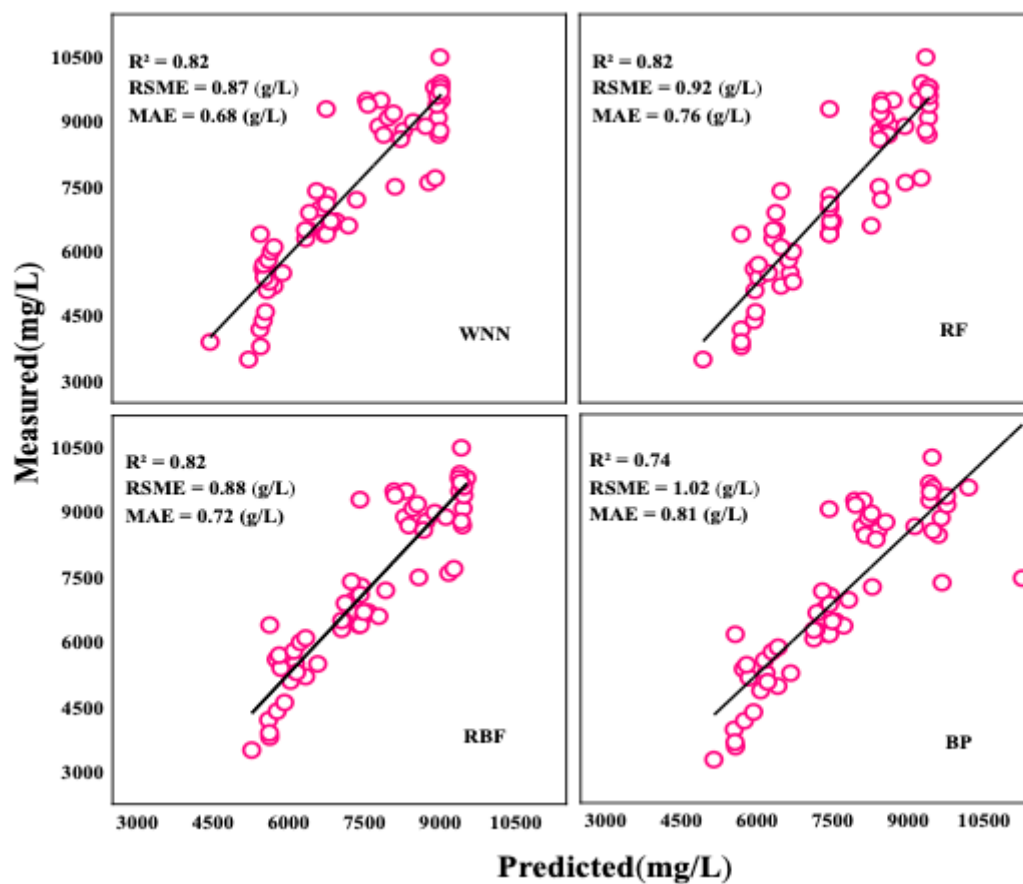
Figure 2

Operation of wavelet neural network

Figure 3

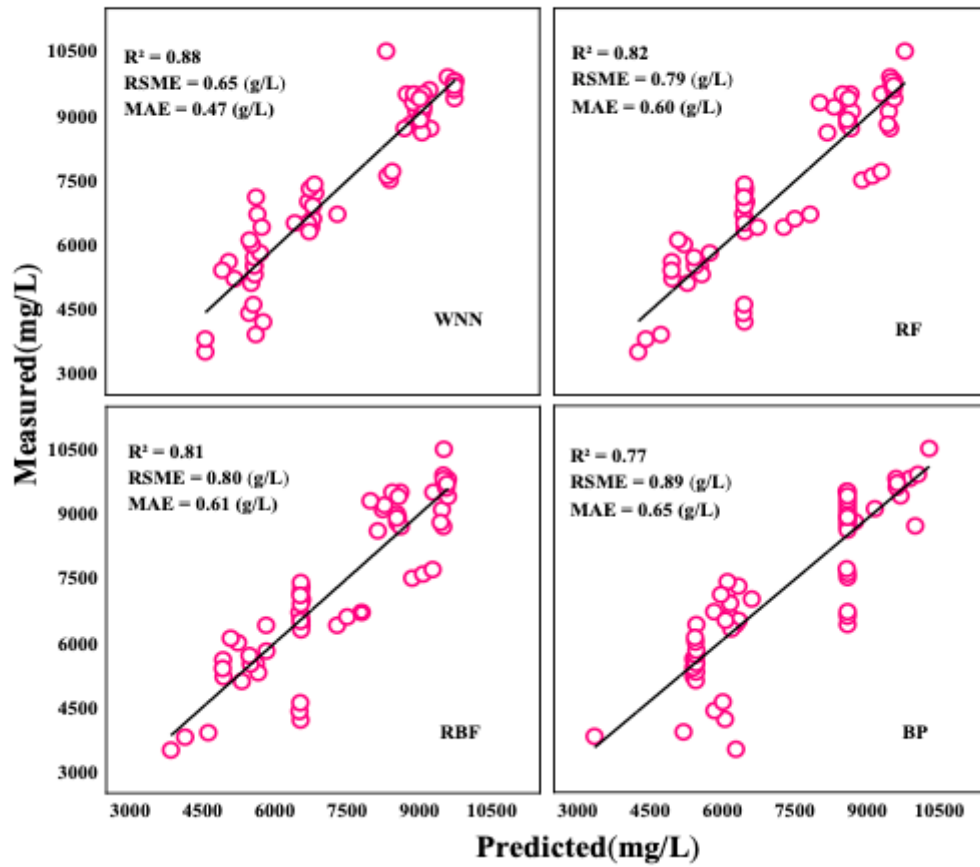Validation of predicted and measured values of NO3--N content in petioles by vegetation indices

Figure 4

Validation of predicted and measured values of NO3--N content in petioles by blue edge parameters